Journal of Photoscience (2001), Vol. 8(1), pp. 27–32

Photoreduction of Methyl Orange Catalyzed by Nile Red-Adsorbed TiO_2 / Y Zeolites using Visible Light

Jeong Jin Lee, Yanghee Kim, Minjoong Yoon*
Department of Chemistry, Chungnam National University, Taejon 305-764, Korea

Photoreduction of Methyl Orange was investigated by using Nile Red-adsorbed TiO_2 / Y zeolites. Nile Red was successfully adsorbed on TiO_2 / Y zeolites and the absorption profile is very broad with maxima, *ca.* 630 nm. The peak is largely red-shifted compared to that observed in hydrocarbon solvents. Furthermore, a broad and largely Stokes shifted emission band as observed around 660 nm. The largely Stokes shifted emission band should be originated from the excited state structural changes. In order to understand the photocatalytic activities of Nile Red-adsorbed TiO_2 / Y zeolite, the photoreduction of Methyl Orange (5.0×10^{-5} M) was studied using visible light beyond 320 nm. Methyl Orange was effectively reduced by Nile Red-adsorbed TiO_2 / Y zeolite, indicating the photocatalytic activity of Nile Red-adsorbed TiO_2 / Y zeolites was enhanced by about eight times higher than that of TiO_2 / Y zeolite.

Key words: photocatalyst, TICT(twisted intramolecular charge transfer), Nile Red, TiO_2 / Y zeolite

INTRODUCTION

Interfacial photochemical reaction on the surface of TiO_2 particles as semiconductor has attracted much interest because of its potentiality in developing high conversion of solar energy into chemical energy, degradation of pollutants, and so on [1-3]. The principal use of small semiconducting particles is as a source of electrons (e^-) and holes (h^+) created by the absorption of light. After excitation of TiO_2, the photogenerated electrons migrate from valence band to conduction band which the generated holes in void site of valence band, followed by their participation in the electron transfer reaction with adsorbed molecules [4]. In competition with this process, however, electron-hole recombination should take place within femtosecond and picosecond regions in a TiO_2 particle [5-8]. For example, Bowman R. M *et al.* have reported that the photogenerated electron of conduction band in the TiO_2 colloidal system become rapidly trapped, and subsequently undergo electron-hole recombination within the first 50 ps [9]. Such a rapid electron-hole recombination diminishes the overall efficiency of photoactive TiO_2 particles.

For the control of electron transfer processes like the quick electron-hole recombination, the preparation of introducing Ti species directly into Y zeolites with large 13 Å supercages connected 7.4 Å windows through the common ion exchange procedures using an aqueous solution of $(NH_4)_2TiO(C_2O_4)_2H_2O$ [10]. To increase the efficiency of TiO_2 particles as photocatalyst, we make an attempt to encapsulate TiO_2 particles in zeolites. Recently, zeolites have been used as hosts to fix semiconductors because they offer unique of reaction fields nanoscaled pores [10-12]. Because the zeolites have void shape-selective cavities and the pores sizes are similar to those of generally organic molecules, these TiO_2 particles encapsulated within Y zeolites isolates the photosensitive organic molecules. Finally, TiO_2/Y zeolites are effective in the utilization of sunlight. In our previous work, we have reported the new photocatalytic system that combine the TiO_2/Y zeolite with ρ-*N,N'* dimethylaminobenzoic acid(DMABA) as an intramolecular charge transfer(ICT) molecule [13]. Through these studies we have found that this photocatalytic system has enhanced the photocatalytic efficiency as well as the recovery efficiency. Nevertheless, DMABA has a limitation to absorb a UV (ultraviolet) light below 320 nm that is no more than 5% of sunlight.

In the present work we attempted to use Nile Red to encapsulate into the TiO_2/Y zeolites to utilize effectively the whole solar light without loss of energy in which particular photoresponse to visible light. Nile Red is an excellent candidate for sensing applications since it is highly solvatochromic, i.e., exhibits wavelength shifts in both absorbance and emission bands in the presence of various molecules [14]. Chemisorption of the sensitization dye on the surface of the wide band gap semiconductors such as titanium dioxide plays an important role in the sensitization efficiency. J. Cherepy *et al.* have designed successfully an efficient and stable solar cell by using semiconductor films consisting of nanometer sized TiO_2 particles and charge transfer dyes [3]. The dye is typically adsorbed on the surface of the semiconductor particles and acts as an electron donor, injecting electrons from the excited state Nile Red into the conduction band of the semiconductor under visible light irradiation. Instead of the TiO_2 particles, we

*To whom correspondence should be addressed.
E-mail : mjyoon@cnu.ac.kr
Received 15 February 2001; accepted 15 March 2001

have used the TiO_2/Y zeolites to support the Nile Red to develop the new photocatalyst responding to the visible light. The new photocatalyst system must be improved in its quantum efficiency, too.

MATERIALS AND METHODS

Material. The HY zeolite was prepared by ion-exchanging with the NaY zeolite(Si/Al = 2.47) with 0.1 M NH_4Cl [15]. Titanium-exchanged zeolites were prepared from HY zeolites with an aqueous solution of ammonium titanyl oxalate monohydrate, $(NH_4)_2TiO(C_2O_4)_2H_2O$ (Aldrich Chemical Co.) as described by Liu, Lu and Thomas [10,15]. The ion-exchanged zeolite has 7.2 Ti species each unit cell. The titanium-exchanged zeolites were washed with the triply distilled water several times to remove the chemicals, which were adsorbed on external surface, and dried with air suction. The sample was then calcinated at 450°C for 6 h. The temperature of the sample was elevated with a rate of 1.67 °C/min. The sample was cooled down by decreasing the temperature with the same rate as the temperature increased. The TiO_2/Y zeolite were transferred to a pyrex cell and activated at 230-240°C for 2 h under vacuum (10^{-4} torr), then shaken with 10 ml of degassed acetonitrile solution containing 1.0×10^{-3} M Nile Red for 12 h. To remove acetonitrile, the solid was dried in vacuum. The dried solid was transferred to quartz cell under the same vacuum for the spectroscopic measurements.

Experimental methods. The X – ray diffractograms were recorded on MO3X-HF diffractometer (Model-1031, Mac Science Co.). To measure the IR spectra, JASCO FT/IR-410 spectrometer and KBr technique were used. Diffuse reflectance UV-vis spectra were recorded by using a Shimadzu UV-3101PC spectrometer equipped with an integrating sphere. Absorption spectra were measured on a SHINCO UVS 2040 spectrometer. Diffuse reflectance fluorescence measurements were made on a scanning SLM – AMINCO 4800 spectrofluorometer, which makes it possible to obtain corrected spectra using Rhodamine B as a quantum counter.

Nile Red-adsorbed TiO_2/Y zeolite or TiO_2/Y zeolite were directly mixed with 5.0×10^{-5} M aqueous Methyl Orange solution under argon gas flow. The mixture samples were split into Pyrex test tubes, and they were irradiated by using merry-go-round equipped with Xe-arc lamp attached with water filter and the cut-off filter transmitting the light longer than 320 nm. After a certain period of irradiation, each irradiated solution was filtered with 0.2 μm PVDF filter for removing Nile Red-adsorbed zeolite and its absorption spectra were measured to monitor the solution of Methyl Orange.

RESULTS AND DISCUSSION

Figure 1(a) shows the X-ray diffraction (XRD) pattern of

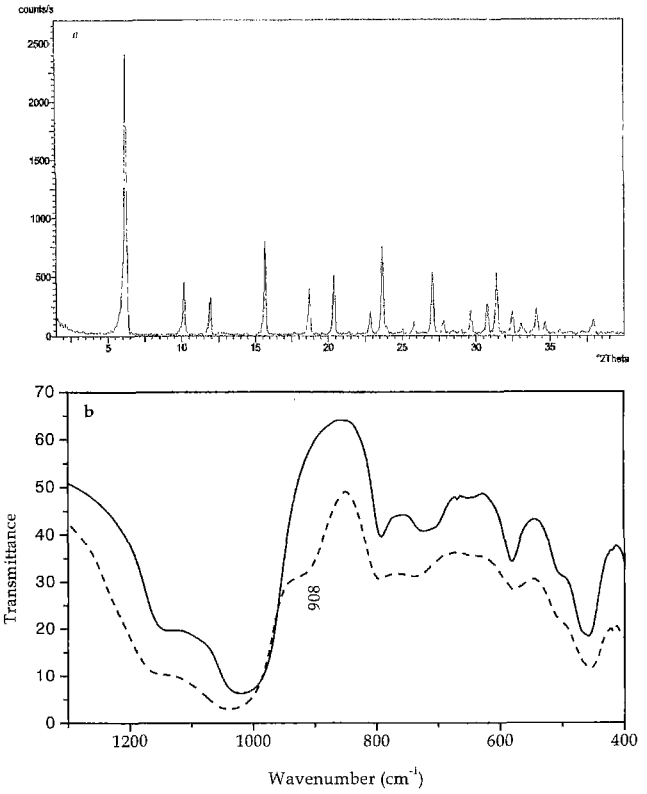

Figure 1. (a) The X-ray diffraction pattern of TiO_2/Y zeolite and (b) the IR spectra of HY and TiO_2/Y zeolite.

TiO_2/Y zeolite was ion exchanged with aqueous solution of ammonium titanyl oxalate mono-hydrate, $(NH_4)_2TiO(C_2O_4)_2H_2O$. The XRD pattern of TiO_2/Y zeolite is well matched with that of HY zeolites. This indicates that the sample doesnít contain an amorphous phase or TiO_2 phase and the framework structure of zeolite is unchanged during the ion exchange process. The titanium species residing in the zeolite cavities or channels are too small to be detected by XRD [10]. Infrared (IR) spectra of TiO_2/Y zeolites show new absorption bands at 920, 895, 860 cm^{-1}. According to Liu *et al.*'s report, the monomer Ti – O and Ti – O stretching vibrations have frequencies of 1087 and 975 cm^{-1}, respectively, and the Ti–O–Ti linkage vibration is around 850 cm^{-1} [15]. This indicates that the TiO^{2+} species as well as Ti–O–Ti linkages are also present in the zeolites. In addition to the new bands at 918, 894 and 859 cm^{-1}, the IR spectra also show a slight shift of the T–O–T or O–T–O (T = Si or Al) stretching vibration of the framework (around 1000 cm^{-1}) toward higher frequency, illustrating the effect of the Ti species on the zeolites framework. Calcination of the samples at 550°C causes overlapping of the new absorption bands in the IR spectra, and the fine structure of the bands is no longer observed. This implies that a further aggregation of the Ti species to form larger particles in the zeolites cavities takes place [10,15]. The TiO_2/Y zeolite shows a broad band around 908 cm^{-1} (Figure 1b). This IR spectral band was matched for with that of

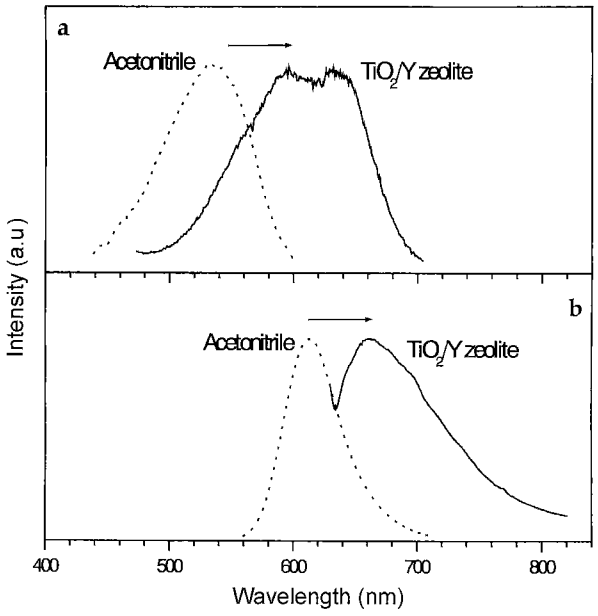

Figure 2. (a) Absorption spectra and (b) Emission spectra of Nile Red in both acetonitrile (dotted line) and TiO_2/Y zeolite (solid line).

previous reports of the titanium-exchanged zeolites Y [13,15]. The TiO_2/Y zeolite exhibits different features in the IR spectrum of the HY zeolite. This phenomenon supports that the direct introduction of the Ti species into zeolites cavities through the ion-exchange procedures.

The diffuse reflectance absorption spectrum of Nile Red-adsorbed TiO_2/Y zeolite is shown in Figure 2(a) with the absorption spectrum of Nile Red in acetonitrile. The absorption spectrum of Nile Red is broad with its band maximum located at 630 nm in TiO_2/Y zeolite and at 535 nm in acetonitrile. The diffuse reflectance spectrum of Nile Red-adsorbed TiO_2/Y zeolite is a little red-shifted from the absorption maximum of Nile Red in acetonitrile. Figure 2(b) shows the emission spectra of Nile Red in acetonitrile and TiO_2/Y zeolite. The emission spectra reveal remarkable changes in the emission band position as a function of medium, as in the case of the absorption spectra. This is probably due to the molecules of Nile Red strongly sensitive to the polarity of their micro-environment. Similar results were observed for Na^+-exchanged Y zeolites [16]. Not only in the supercages of zeolite they can be characterized as superpolar (the supercages are much more polar than all organic solvents) but also in the organic solvent, respectively which agree with reported results; for example, the absorption band maximum shift from 488 nm in hexane to 565 nm in methanol and the corresponding emission shifts from 525 nm in hexane to 625 nm in methanol [17]. Such large shifts in the absorption and emission band maxima may be attributed to the large excited state dipole moment of the molecule in polar media.

Nile Red exhibits nearly complete charge separation between the diethylamino group which acts as an electron donor and quinoid part of the molecule which is the electron acceptor

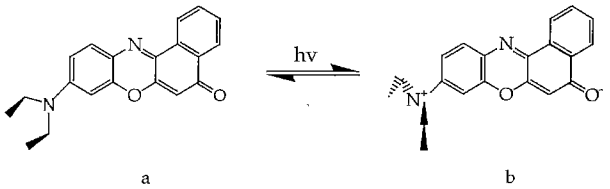

Scheme 1. Nile red structural formulas : (A) planar and (B) twisted.

due to the rotation of the flexible diethylamino group attached to the rigid structure of the molecule [18-20] (Scheme 1). The charge separation may be explained by the formation of the twisted intramolecular charge transfer (TICT) of molecule in polar solvents. The excitation spectra of Nile Red monitored at the two emission maxima reveal two distinct peaks in methanol-water (binary mixture): the distinct differences between the band position provide that the bands originate from completely different species or configurational states, which is in agreement with the TICT model [18]. 4-*N,N'*-dimethylaminobenzonitrile(DMABN) is one of the TICT molecules which show dual fluorescence in polar solvents: a large Stokes' shifted emission of the excited TICT state in addition to the normal emission from the local excited state. Unlike DMABA, Nile Red shows only single broad emission band in pure polar solvent (Figure 2b) by efficient energy transfer from the higher configurational energy state to the lower configurational energy state [18,19]. This indicates that Nile Red encapsulated within TiO_2/Y zeolite exist in TICT state in which wholly photoinduced charge separation occurs.

To confirm the superpolarity of supercages, we attempted to measure the fluorescence lifetime of the Nile Red-adsorbed TiO_2/Y zeolites. Figure 3 shows typical temporal profile of fluorescence decay for the Nile Red-adsorbed TiO_2/Y zeolite.

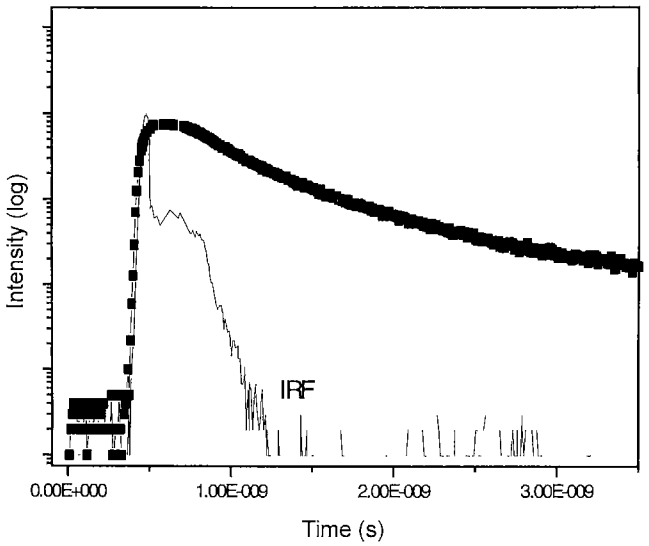

Figure 3. The fluorescence decay profile of the normal emission of Nile Red-adsorbed TiO_2/Y zeolite monitored at 660 nm. The excitation wavelength is 580 nm.

The transition of Nile Red from the excited singlet state to the fluorescence TICT state is so fast that the rise of the fluorescence intensity is not observed [18,21]. For the Nile Red-adsorbed TiO_2/Y zeolites, TICT emission decays with the two decay times (1.6 ns, 380 ps). The 1.6 ns decay component is attributed to the emission from stabilized TICT state while 380 ps component corresponds to the rotational reorientation time(τ_r). The one decay time (1.6 ns) is remarkable contrast to those for the TICT emission measured in various solutions. For example, the fluorescence lifetime of Nile Red is 3.6 ns in ethanol and 5.1 ns in CCl_4 [21]. This indicates that fluorescence lifetime decreased with increase in the polarity of the medium. This comparison leads to the conclusion that the relatively short fluorescence lifetime of Nile Red in TiO_2/Y zeolites as compared to that in all organic solvents is attributable to the high polarity of zeolite cavities.

Unlike other TICT molecules, Nile Red in TiO_2/Y zeolite shows only single fluorescence corresponding to the TICT state of completely charge seperation. This indicates that the photochemical electron transfer between Nile Red and TiO_2/Y zeolite could be progressed efficiently more than DMABA in TiO_2/Y zeolite. The photochemical interaction should be caused by an electron transfer from Nile Red to the conduction band of TiO_2 attached inside the nanopore frame of the zeolite. The photoinduced electron transfer from the exited singlet state of DMABA to TiO_2 conduction band has been previously observed from DMABA-adsorbed TiO_2/Y zeolites [13]. However, the photochemical interaction should be the electron transfer from the excited TICT state of Nile Red to TiO_2 conduction in this photocatalytic system of Nile Red-adsorbed TiO_2/Y zeolite. This could result in enhancement of electron transfer efficiency to the frame of TiO_2/Y zeolite, and the electron subsequently should be accessible for reduction of some other substrate outside the zeolite.

In order to confirm the above speculation, we attempted to observe the photocatalytic activities of the Nile Red-adsorbed TiO_2/Y zeolite by monitoring the photoreduction of Methyl Orange (5.0×10^{-5} M) in aqueous solution. Figure 4 shows the UV-vis spectra of Methyl Orange before and after irradiation ($\geq$ 320 nm) in the presence of Nile Red-adsorbed TiO_2/Y zeolite. Methyl Orange itself in the absence of TiO_2/Y zeolite was photochemically inert as observed by no change in the absorption spectrum. Furthermore, methyl orange and Nile Red mixture was also photochemically inert. However, in the presence of Nile Red-adsorbed TiO_2/Y zeolite, the absorption spectrum of Methyl Orange was significantly changed (Figure 4). The visible absorption band of methyl orange disappears in at 460 nm and a new peak grows in at 247 nm, which was originated from photoreduction product, hydrazine derivative [22]. The spectral change of Methyl Orange solution was also observed by irradiating in the presence of free TiO_2/Y zeolite, but the bleaching is very weak. This indicates that light absorbed TiO_2 as well as Nile Red will lead to destruction of Methyl Orange. Furthermore, no absorption spectral shift was

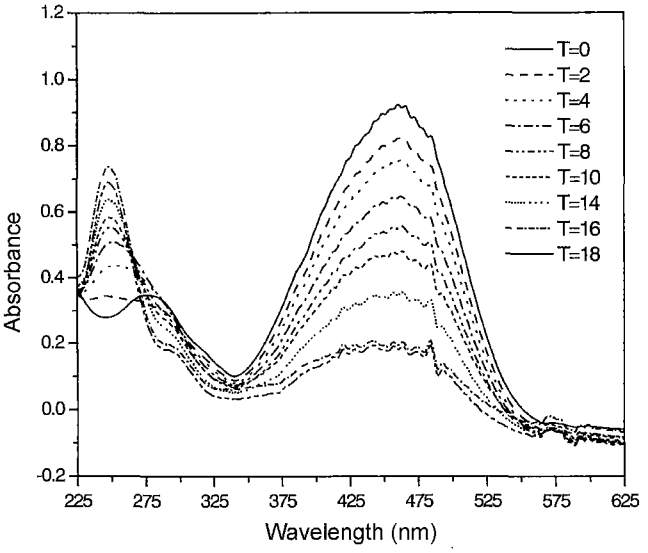

Figure 4. Absorption spectral change of the filtered solution of Methyl Orange after irradiation in the presence of Nile Red-adsorbed TiO_2/Y zeolites. Concentration of Methyl Orange was 5.0×10^{-5} M. The irradiation wavelength is longer than 320 nm. 'T' stand for the irradiation times (minutes).

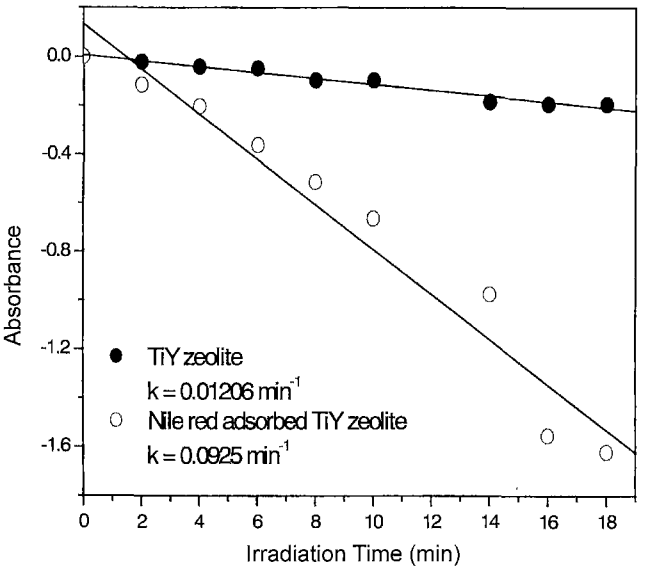

Figure 5. Plot of the absorption change of Methyl Orange 460 nm as a function of irradiation time in the presence of Nile Red-absorbed TiO_2/Y zeolite(○), and free TiO_2/Y zeolite (●).

observed at 460 nm, indicating the Methyl Orange could be reduced by Nile Red-adsorbed TiO_2/Y zeolite and free TiO_2/Y zeolite. These results imply that the photoreduction of Methyl Orange is catalyzed by the TiO_2/Y zeolite. Figure 5 shows the degree of the bleaching of methyl orange as a function of irradiation time. This exhibits the photocatalytic activity of Nile Red-adsorbed TiO_2/Y zeolite about eight times higher than free TiO_2/Y zeolite, indicating that Nile Red-adsorbed on TiO_2/Y zeolite plays an important role in increasing the

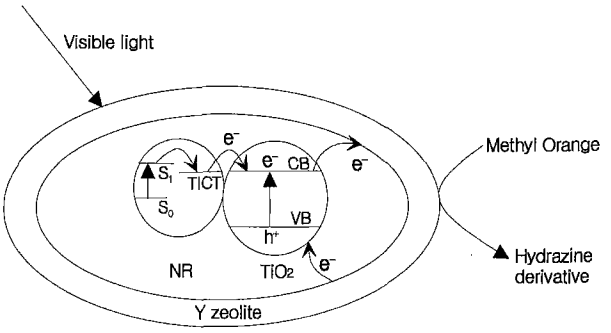

Scheme 2.

photocatalytic activity of TiO_2/Y zeolite.

The photoreduction of Methyl orange is shown in Scheme 2 involving accepting electron transport through the TiO_2/Y zeolite frame. Upon irradiation of TiO_2 on TiO_2/Y zeolite by UV light, the conduction band electron can be removed quickly from the TiO_2 site before charge recombination, because the electron-rich zeolite surface function as a hole scavenger [23]. This is the reason why the free TiO_2/Y zeolite catalyzes the photoreduction of Methyl orange, even though the efficiency is low (<10%). However, in the Nile Red-adsorbed TiO_2/Y zeolite, Nile Red also absorbs visible light used to induce electron transfer from the excited TICT state of Nile Red to TiO_2 on the TiO_2/Y zeolite. Consequently, the electron density in conduction band of TiO_2 on the zoelite is increased as compared to the free TiO_2/Y zeolite. The excess conduction band electrons of TiO_2 on the zeolite frame could be transported through more efficiently than the case of free TiO_2/Y zeolite.

CONCLUSION

The Nile Red can be entrapped into the nanopores of TiO_2/ Y zeolite, playing an important role in enhancement of electron density on the conduction photocatalytic activity of TiO_2/Y zeolite for the reduction of organic compounds in water. Furthermore, it should be also noted that the Nile Red-adsorbed TiO_2/Y zeolite could be successfully recovered by filtration and reused as the photocatalyst. Therefore, this photocatalyst would be very useful for the cleaning of wastewater containing organic compounds because Nile Red absorb the visible light, the most available sunlight.

REFERENCES

1. Andrew Mills and Stephen hunte (1997) An overview of semiconductor photocatalysis: *J. Photochem. Photobiol. A*, **108**(1), 1-35.
2. Jianjun He, Jincai Zhao, Tao Shen, Hisao Hidaka and Nick Serpone (1997) Photosensitization of colloidal titania particles by electron injection from an excited organic dye-antennae function: *J. Phys. Chem. B,* **101**, 9027-9034.
3. Nerine J. Cherepy, Gerg P. Smestad, Michael Grätzel and Jin Z. Zhang (1997) Ultrafast electron injection: Implications for a photoelectrochemical cell utilizing an anthocyanin dye-sensitized TiO_2 nanocrystalline electrode, *J. Phys. Chem. B,* **101**, 9324-9351.
4. Akihiro Furube, Tsuyoshi Asahi, Hiroshi Mashtara, Siromi Yamashita and Masakazu Anpo (1999) Charge carrier dynamics of standard TiO_2 catalysts revealed by femtosecond diffused reflectance spectroscopy: *J. Phys. Chem. B*, **103**, 3120-3127.
5. Guido Rothenberger, Jacques Moser, Michael Grätzel, Nick Serpone and Devendra K. Sharma (1985) Charge carrier trapping and recombination dynamics in small semiconductor particles: *J. Am. Chem. Soc.*, **107**, 8054-8059.
6. David E. Skinner, D. Philip Colombo, Jr., Joseph J. Cavaleri and Robert M. Browman (1995) Femtosecond investigation of electron trapping in semiconductor nanoclusters: *J. Phys. Chem.*, **99**, 7853-7856.
7. N. Serpone, D. Lawless, R. Khairutdinov and Ezio Pelizzetti (1995) Subnanosecond relaxation dynamics in TiO_2 colloical sols (Particle Sizes R_p = 1.0-13.4 nm). Relevance to heterogeneous photocatalysis: *J. Phys. Chem.*, **99**, 16655-16661.
8. Gopidas, K. R. Maria Bohorquez and Prashant V. Kamat (1990) Photophysical and photochemical aspects of coupled semiconductors charge-transfer processes in colloidal CdS-TiO_2 and CdS-AgI systems: *J. Phys. Chem.*, **94**, 6435-6440.
9. Colombo, D. Philip Jr., Kirsten A. Roussel, Jamal Saeh, David E. Skinner, Joseph J. Cavaleri and Robert M. Bowman (1995) Femtosecond study of the intensity dependence of electron-hole dynamics in TiO_2 nanoclysters; *Chem. Phys. Lett.*, **232**, 207-214.
10. Xinsheng Liu, Kai-Kong lu and J. kerry Thomas (1993) Preparation, characterization and photoreactivity of titanium (IV) oxide encapsulated in zeolites: *J. Chem. Soc., Faraday Trans.*, **89**(11), 1861-1865.
11. Masakazu Anpo, Hiromi Yamashita, Yuichi Ichihashi, Yo Fujii and Miwa Honda (1997) Photocatalytic reduction of CO_2 with H_2O on titanium oxides anchored within micropores of zeolites: Effects of the structure of the active sites and the addition of Pt: *J. Phys. Chem. B*, **101**, 2632-2636.
12. Hiromi Yamashita, Yuichi Ichihashi, Masakazu Anpo, Mitsuo Hashimoto, Catherine Louis and Michel Che (1996) Photocatalytic decomposition of NO at 275 K on titanium oxides included within Y-zeolite cavities: The structure and role of the active sites: *J. Phys. Chem.*, **100**, 16041-16044.
13. Yanghee Kim and Minjoong Yoon (2000) TiO_2/Y-Zeolite encapsulation intramolecular charge transfer molecules: A new photocatalyst for photoreduction of methyl orange in aqueous medium: *J. Mol. Catal. A: Chem.*, **168**, 257-263.
14. Julia L. Meinershagen and Thomas Bein (1999) Optical sensing in nanopores. Encapsulation of the solvatochromic dye nile red in zeolites: *J. Am. Chem. Soc.*, **121**, 448-449.
15. Xinsheng Liu, Kai-Kong Iu and J. Kerry Thomas (1992) Encapsulation of TiO_2 in zeolites Y: *Chem. Phys. Lett.*, **195**, 163-168.
16. Yanghee Kim, Byeong In Lee and Minjoong Yoon (1998)

Excite-state intramolecular charge transfer of ρ - *N*, *N*-dimethylaminobenzoic acid in Y zeolites: hydrogen-bonding effects: *Chem. Phys. Lett.*, **286**, 466-472.
17. Sundararajan Uppili, K. J. Thomas, Elizabeth M. Crompton and V. Ramamurthy (2000) Probing zeolites with organic molecules: Supercages of X and Y zeolites are superpolar: *Langmuir*, **16**, 265-274.
18. Ashim Kumar Dutta, Kenji Kamada and Koji Ohta (1996) Spectroscopic studies of nile red in organic solvents and polymers: *J. Photochem. Photobiol. Chem.*, **93**, 57-64.
19. Nagwa Ghoneim (2000) Photophysics of nile red in solution steady state spectroscopy: *Spectrochim. Acta Part A.* **56**, 1003-1010.
20. Ashim Kumar Dutta, Kenji Kamada and Koji Ohta (1996) Langmuir-Blodgett films of nile red: a steady-state and time-resolved fluorescence study: *Chem. Phys. Lett.*, **258**, 369-375.
21. Myungjin Choi, Daeseong Jin and Hackjin Kim (1997) Fluorescence anisotropy of nile red and oxazine 725 in an isotropic liquid crystal: *J. Phys. Chem. B*, **101**, 8092-8097.
22. Brown, G. T. and Darwent, J. R. (1984) Photoreduction of methyl orange sensitized by colloidal titanium dioxide: *J. Chem. Soc., Faraday Trans. I*, **180**, 1631-1643.
23. Anpo, M., Yamashita, H., Ichihashi, Y., Fujii, Y. and Honda, M. (1997) Photocatalytic reduction of CO_2 with H_2O on titanium oxides anchored within micropores of zeolites: Effects of the structure of the active sites and the addition of Pt: *J. Phys. Chem. B*, **101**, 2632-2639.